

Treatment and Resource Recovery

In-situ-generated reactive oxygen species in pre-charged titania and tungsten trioxide composite catalyst membrane filters: Application to As(III) oxidation in the absence of irradiation

Jiyeon Park, Jonghun Lim, Yiseul Park, Dong Suk Han, Hokyong Shon, Michael R Hoffmann, and Hyunwoong Park

Environ. Sci. Technol., **Just Accepted Manuscript** • DOI: 10.1021/acs.est.0c01550 • Publication Date (Web): 16 Jun 2020

Downloaded from pubs.acs.org on June 16, 2020

Just Accepted

“Just Accepted” manuscripts have been peer-reviewed and accepted for publication. They are posted online prior to technical editing, formatting for publication and author proofing. The American Chemical Society provides “Just Accepted” as a service to the research community to expedite the dissemination of scientific material as soon as possible after acceptance. “Just Accepted” manuscripts appear in full in PDF format accompanied by an HTML abstract. “Just Accepted” manuscripts have been fully peer reviewed, but should not be considered the official version of record. They are citable by the Digital Object Identifier (DOI®). “Just Accepted” is an optional service offered to authors. Therefore, the “Just Accepted” Web site may not include all articles that will be published in the journal. After a manuscript is technically edited and formatted, it will be removed from the “Just Accepted” Web site and published as an ASAP article. Note that technical editing may introduce minor changes to the manuscript text and/or graphics which could affect content, and all legal disclaimers and ethical guidelines that apply to the journal pertain. ACS cannot be held responsible for errors or consequences arising from the use of information contained in these “Just Accepted” manuscripts.

In-situ-generated reactive oxygen species in pre-charged titania and tungsten trioxide composite catalyst membrane filters: Application to As(III) oxidation *in the absence of irradiation*

Ji Yeon Park,^{a,ψ} Jonghun Lim,^{b,ψ} Yiseul Park,^c Dong Suk Han,^d Ho Kyong Shon,^e Michael R. Hoffmann,^b and Hyunwoong Park^{a,*}

^a *School of Energy Engineering, Kyungpook National University, Daegu 41566, Korea*

^b *Linde + Robinson Laboratories, California Institute of Technology, Pasadena, California 91125, United States*

^c *Department of Chemical Engineering, Pukyong National University, Busan 48513, Korea*

^d *Center for Advanced Materials, Qatar University, Doha 2713, Qatar*

^e *Centre for Technology in Water and Wastewater, School of Civil and Environmental Engineering, University of Technology Sydney, Australia*

* To whom correspondence should be addressed (H. Park)

E-mail: hwp@knu.ac.kr; Tel: +82-53-950-8973

^ψThese authors contributed equally to this work.

Keywords

Solar charging; Reactive oxygen species; Composites; Membrane filters; Charge storage

Abstract

This study demonstrates that in situ-generated reactive oxygen species (ROSs) in pre-photocharged TiO_2 and WO_3 (TW) composite particle-embedded inorganic membrane filters oxidize arsenite (As(III)) into arsenate (As(V)) without any auxiliary chemical oxidants under ambient conditions in the dark. TW membrane filters have been charged with UV or simulated sunlight and subsequently transferred to a once-through flow-type system. The charged TW filters can transfer the stored electrons to dissolved O_2 , producing ROSs that mediate As(III) oxidation in the dark. Dramatic inhibition of As(V) production with O_2 removal or addition of ROS quenchers indicates an ROS-mediated As(III) oxidation mechanism. Electron paramagnetic spectroscopic analysis has confirmed the formation of the $\text{HO}_2^\bullet/\text{O}_2^{\bullet-}$ pair in the dark. The WO_3 fraction in the TW filter significantly influences the performance of the As(III) oxidation, while As(V) production is enhanced with increasing charging time and solution pH. The As(III) oxidation is terminated when the singly charged TW filter is fully discharged; however, recharging of TW recovers the catalytic activity for As(III) oxidation. The proposed oxidation process using charged TW membrane filters is practical and environmentally benign for the continuous treatment of As(III)-contaminated water during periods of unavailability of sunlight.

Introduction

Photocatalytic water treatment has been extensively studied over the last few decades and has proven to be capable of remediating most (in)organic chemicals via redox reactions.¹⁻ Recently, the practical applicability of photocatalytic systems in the near future compared to other competitive analogues (UV with H₂O₂ and/or O₃) in terms of efficiency, durability, and costs for material and system has been debated.⁴ Heterogeneous oxide photocatalysts (e.g., TiO₂, ZnO, and WO₃) may exhibit a lower photo-efficiency than the UV-based homogeneous ones. However, the former works directly under natural sunlight whereas the latter essentially requires electricity (UV light) and auxiliary chemicals (H₂O₂, O₃, etc.). Although the photocatalyst materials are relatively cheap (e.g., ~\$1 per kg for TiO₂) and durable,⁴ they become more expensive and less durable when coupled with expensive, secondary materials (e.g., noble metals, graphenes, and polymers).²⁻³ Post-recovery steps of used, suspended particles largely increase the operation cost of the photocatalytic system. More importantly, the periodic and abrupt fluctuations of sunlight further limit continuous operation of the system. All these factors make the photocatalysis less applicable as an independent process, inevitably requiring additional treatments.

With this in mind, we have long attempted to identify the functionality of particulate TiO₂ and WO₃ composite (TiO₂/WO₃, TW) films and apply them to energy production⁵ and environmental cleanup.⁶⁻⁸ In addition to their synthesis being simple and straightforward, TW films can work *without* i) any auxiliary, expensive materials, ii) post-separation process, and iii) even continuous sunlight. The last function is particularly unique in WO₃ that can store photogenerated electrons (photocharging process) and induce reduction in the following dark periods (discharging process).⁷⁻¹¹ Although TiO₂ itself also can act as an electron reservoir,¹²⁻

¹⁴ the interfacial electron transfer occurs quickly during the photocharging periods under oxidic conditions and the application under the oxidic conditions in the following dark periods is limited. On the other hand, inter-particle contact between WO_3 and other semiconductors with higher conduction bands (e.g., TiO_2 and CdS) significantly shortens the photocharging time due to additional electron supply via cascaded electron transfer while increasing the lifetime of stored electrons.⁷⁻⁸ As-photocharged TW films have been successfully demonstrated to reductively convert metal ions (Cr^{6+} and Ag^+) and organic chemicals (e.g., methylene blue) with the stored electrons in the dark periods.^{6-8,15}

We noted that the stored electrons can be transferred to dissolved O_2 followed by the production of reactive oxygen species (ROSs, e.g., $\text{O}_2^{\bullet-}$, HO_2^{\bullet} , and H_2O_2) which are capable of oxidizing substrates via a reductive pathway (**Scheme 1**). O_2 is the most ubiquitous electron acceptor in aqueous media. In addition, ROSs are environmentally clean oxidizing agents widely used in the treatment of (in)organic substrates.³ This study attempted to apply the TW membrane filters to the oxidation of As(III) to As(V) by ROSs produced via a reductive pathway in the absence of any auxiliary chemicals under ambient conditions in the dark. To the best of our knowledge, this application has not been reported yet. Arsenic-contaminated drinking water has long caused serious problems such as skin lesions and skin cancer to human, particularly in developing countries with limited access to water treatment facilities.¹⁶⁻¹⁷ Arsenite (As(III), H_3AsO_3 ; $pK_a = 9.4, 12.1, \text{ and } 13.4$) is more toxic and difficult for removal than arsenate As(V) (H_3AsO_4) due to higher mobility and lower affinity for absorbents and coagulants in the former.¹⁸⁻¹⁹ Although the photocatalytic As(III) oxidation mechanism should primarily follow an oxidative pathway with hydroxyl radicals ($^{\bullet}\text{OH}$) generated via the hole transfer, the reductive pathway mediated with ROSs has been proposed

to occur as well under irradiation.²⁰ In this study, the hole transfer (*i.e.*, $\bullet\text{OH}$ -mediation) was not directly involved in the discharging process and hence the reductive pathway with the stored electrons (*i.e.*, ROS mediation) should be predominant in the As(III) oxidation. This finding can further support the existence of a reductive pathway in the As(III) oxidation mechanism, which has long been debated.²⁰

Experimental methods

Chemicals and materials. The following chemicals were used in this study: NaAsO₂ (As(III), Sigma-Aldrich), Na₂HAsO₄·7H₂O (As(V), Sigma-Aldrich), molybdate reagent solution (Sigma-Aldrich), methanol (MeOH, Merck), *p*-benzoquinone (BQ, Sigma-Aldrich), hydrochloric acid (Junsei), L-histidine (Sigma-Aldrich), superoxide dismutase (SOD, Sigma-Aldrich; from bovine erythrocytes), ascorbic acid (Sigma-Aldrich), ethanol (Merck), sodium hydroxide (Sigma-Aldrich), hydrogen peroxide (Duksan), SiO₂ (Sigma-Aldrich), WO₃ (Kanto, particle size of ~30 μm), and TiO₂ (Degussa P25 with a primary particle size of approx. 30 nm). All chemicals were of analytical grade and used as received. Ultrapure deionized water (18 MΩ cm) was used to prepare all aqueous solutions.

Preparation of photocharged membrane filters. To make composite TiO₂ and WO₃ (TW) particle-embedded membrane filters, TiO₂ and WO₃ particles were suspended in air-equilibrated aqueous solutions with ethanol (20 vol%) as a hole scavenger in TiO₂/WO₃ weight ratios of 1/0, 3/1, 1/1, 1/3, and 0/1 (denoted as TW100, TW75, TW50, TW25, and TW0, respectively) and stirred for 30 min. The suspension was filtered and washed and transferred to a mixed cellulose ester membrane filter (Merck, diameter: 47 mm, pore size: 0.45 μm, thickness: 150 μm) by vacuum filtration. The as-prepared thickness of TW filters

was estimated to be ~0.14 mm using a digital Vernier Caliper (Mitutoyo). The TW membrane was then irradiated (i.e., photocharged) with UV254 (SANYO, G6T5), UV365 (SANKYO, F6T5BLB), and air mass (AM) 1.5 light with an intensity of 100 mW cm^{-2} (1 sun; ABET) for varying times (0.5–5 h; typically, it was 1 h unless otherwise mentioned). The irradiation led to color change from green to dark blue and red-shift of the absorption edge (**Figure S1**), which is consistent with the results obtained in a previous study.⁷

Arsenic redox reaction and characterization. The photocharged TW membrane filters (typically, TW50 unless otherwise mentioned) were transferred to a filtration system for oxidizing As(III) to As(V) (**Figure S2**). Air-equilibrated aqueous As(III) solutions (typically, 0.1 mM in 90 mL at pH 5) passed through the charged TW filters at a flow rate 0.5 mL min^{-1} over 2 h using a peristaltic pump (Longer) in the absence of any irradiation. To examine the effect of dissolved O_2 , N_2 gas was used to purge the feed solutions prior to and during the flow process. If necessary, pH of the feed solutions was initially adjusted using HCl and NaOH to examine the effect of pH on the As(III) oxidation kinetics. The filtered solutions were intermittently sampled and analyzed for As(V) concentrations (i.e., $[\text{As(V)}]$), which were then converted into the amounts of As(V) ($= [\text{As(V)}]_t \times \text{flow rate} \times t$; where t is time). $[\text{As(V)}]_t$ in the filtered solution was colorimetrically determined using molybdenum blue method.²¹ In brief, 0.5 mL of the aliquot was added to a conical tube containing deionized water (2.2 mL), ascorbic acid (100 μL at 0.1 g mL^{-1}), and a molybdate reagent solution (200 μL , Sigma-Aldrich). The mixed solution was vigorously mixed and kept in an oven for 2 h at 40°C ; then, it was analyzed using a UV-visible spectrophotometer (Shimadzu, UV-2450) at $\lambda = 870 \text{ nm}$ ($\epsilon = 19,550 \text{ M}^{-1} \text{ cm}^{-1}$).²¹ In addition, an As(V) solution (instead of As(III)) passed through the charged TW and the amounts of As(III) produced via reduction of As(V)

were quantified using a high-performance liquid chromatography (HPLC, Waters 2695) instrument equipped with a Aminex HPX-87H ion exclusion column (Bio-Rad, 300×7.8 mm) and a dual absorbance detector (Waters 2487). A binary mixture of distilled water and sulfuric acid (5 mM) was used as a mobile phase at a flow rate of 0.6 mL min^{-1} . For comparison, the redox behavior of Cr(VI/III) pair with the charged TW membrane filters was examined (**Figure S3**).

The pore structures of the as-prepared TW samples were analyzed using a gas sorption analyzer (Autosorb-iQ & Quadrasorb SI, Quantachrome Instrument). The Brunauer-Emmett-Teller (BET) surface area of the TW composite particles was estimated to be $33.87 \text{ m}^2 \text{ g}^{-1}$, and their average pore diameter and volume were 27.15 nm and 0.23 cc g^{-1} , respectively. The surface charge of the samples was also analyzed at pH 5 using an electrophoretic light scattering system (Zetasizer Nano ZS, Malvern). The zeta potentials of TiO_2 , WO_3 , and TiO_2/WO_3 particles were estimated to be +22.1, -29.4, and -20.1 mV, respectively. The diffuse reflectance (R) spectra of TW before and after photocharging was obtained using the spectrophotometer (Shimadzu, UV-2540) and converted into the absorbance using the Kubelka-Munk equation ($\text{Abs} = (1-R)^2/2R$). Time-resolved photoluminescence lifetime (TRPL) decays of non-charged and charged TW filters were obtained using a confocal microscope (MicroTime-200, Picoquant, Germany) with a $40\times$ objective. The lifetime measurements were performed at the Korea Basic Science Institute (KBSI), Daegu Center, Korea. A single-mode pulsed diode laser (375 nm with 30 ps pulse width and 3–5 μW power) was used as an excitation source. Details of the analysis have been reported elsewhere.²²⁻²³ Electron paramagnetic resonance (EPR) analysis was performed using 5,5-dimethyl-1-pyrroline *N*-oxide (DMPO, >97%, TCI) as the spin-trapping reagent for

OH[•] and O₂^{•-} (or HO₂[•]). The EPR spectrometer (Bruker EMXplus-9.5/2.7) was operated with a center field of 3,360 G, microwave frequency of 9.430 GHz, microwave power of 6.325 mW, modulation frequency of 100 kHz, and modulation amplitude of 5 G.

The maximum photon-to-charge storage efficiency (ϕ_{ps}), stored charge-to-As(III) oxidation efficiency (ϕ_{sc}), and overall photoconversion efficiency (ϕ_{pc} , *i.e.*, in the dark) were estimated as follows (Eqs. 1-4).

$$\phi_{ps} = \text{number of stored charges/number of incident photons} \times 100\% \quad (\text{Eq. 1})$$

$$\phi_{sc} = \text{number of As(V) produced/number of stored charges} \times 100\% \quad (\text{Eq. 2})$$

$$\phi_{pc} = \text{number of As(V) produced/number of incident photons} \times 100\% \quad (\text{Eq. 3})$$

$$\phi_{pc} = \phi_{ps} \times \phi_{sc} \quad (\text{Eq. 4})$$

The number of incident photons from UV254 was estimated using a well-known chemical actinometer couple of iodide and iodate (assuming a quantum yield of 75%).²⁴ In addition, the maximum storage capacity of WO₃ was assumed to be 115 mAh g⁻¹ when a single charge was stored as in the form of HWO₃.²⁵ TiO₂ was considered incapable of storing charges.

Results and discussion

Catalytic oxidation of As(III) using charged TW membrane filters. As-fabricated TW membrane filters were pre-irradiated for 1 h using three different lamps (UV254, UV365, and AM1.5) and transferred to a once-through flow-type system for redox reactions of As(V/III) pair in the dark (**Figure S2**). As air-equilibrated As(V) solution passed through the TW filter pre-charged with UV254, the maximum amount of As(III) ($[\text{As}^{\text{III}}]_{\text{max}}$) of ~0.2 μmol was produced in 1 h in the filtered solution (**Figure 1a**).

N₂-purging of the As(V) solution enhanced the As(III) production by two times. The reduction of As(V) to As(III) is attributed to the well-known electron transfer from the charged TW to the As(V) (**R1**, where e^-_{TW} refers to stored electrons in the charged TW).

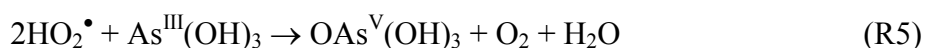
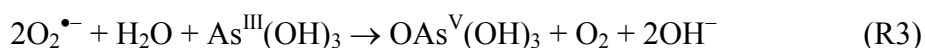


Such charge transfer should be facilitated with N₂ purging due to the removal of the competing O₂ for the electron (i.e., $E^\circ[\text{As(V/III)}] = \sim +0.26$ V at pH 5; $E^\circ(\text{O}_2/\text{HO}_2^\bullet) = -0.05$ V).²⁶

Notably, when air-equilibrated As(III) solutions (*instead of As(V)*) were passed through the charged TW, As(V) was continuously produced with a $[\text{As}^{\text{V}}]_{\text{max}}$ of ~ 0.15 μmol in 3 h in the absence of irradiation (**Figure 1b**). A similar time profile of As(V) production (but with a smaller $[\text{As}^{\text{V}}]_{\text{max}}$) was observed for the UV365-charged TW. Photocharging with AM1.5 light (100 mW cm⁻²) led to the same $[\text{As}^{\text{V}}]_{\text{max}}$ as the that for UV254 despite slower kinetics. This indicates that the pre-charged TW membrane filters can be used *not only for As(V) reduction but also for As(III) oxidation in the dark*, regardless of the irradiation condition, as long as the TW is charged (*see below for more discussion*). As(V) was not produced with non-charged TW filters, indicating that the pre-charging is essential for As(III) oxidation. It is noteworthy that the As(V) production was markedly inhibited with N₂ purging, whereas it was enhanced with O₂ purging ($[\text{As}^{\text{V}}]_{\text{max}} \sim 0.2$ μmol). This phenomenon is in contrast to the case of reduction of As(V) to As(III) (**Figure 1a**). Dissolved O₂ appears to mediate As(III) oxidation via various reactive oxygen species (ROs) produced by the stored electrons. It should be noted that the contradictory role of O₂ in the As(V/III) redox reaction was not found in the case of Cr(VI/III). As shown in **Figure S3**, the reduction of Cr(VI) to

Cr(III) proceeded faster with N₂ purging than that with air, whereas the oxidation of Cr(III) to Cr(VI) hardly occurred both under N₂-purged and air-equilibrated conditions.

To speculate the ROSs responsible for the As(III) oxidation, air-equilibrated As(III) solutions with methanol (MeOH), *L*-histidine, superoxide dismutase (SOD), and *p*-benzoquinone (BQ) as scavengers of OH• ($k = 3 \times 10^9 \text{ M}^{-1} \text{ s}^{-1}$),²⁷ ¹O₂ ($k = 3 \times 10^7 \text{ M}^{-1} \text{ s}^{-1}$), O₂•⁻ ($k = 1 \times 10^9 \text{ M}^{-1} \text{ s}^{-1}$),²⁸ and HO₂• ($k = 2 \times 10^9 \text{ M}^{-1} \text{ s}^{-1}$),²⁴ respectively, were passed through the charged TW filters (**Figure 2a**). The effects of MeOH and *L*-histidine on the As(V) production were insignificant, whereas the As(V) production was completely inhibited with SOD and BQ. Accordingly, the observed As(III) oxidation was presumed to proceed via the mediation of HO₂•/O₂•⁻ pairs (**R2-R5**).



Interestingly, a thermochemical comparison between the O₂ reduction potential ($E^0(\text{O}_2/\text{O}_2^{\bullet-}) = -0.33 \text{ V}$; $E^0(\text{O}_2/\text{HO}_2^{\bullet}) = -0.05 \text{ V}$)²⁹⁻³⁰ and the CB edge of WO₃ (*approx.* +0.4 V, being more positive than TiO₂ at -0.1 V)^{5,7} indicates that the above reactions are unlikely to occur (**Scheme 1**). However, the reduction potential of adsorbed O₂ can be different from that of free O₂. Even if the difference is not large enough and the CB edge of WO₃ (i.e., defect-free) is still unable to produce HO₂•/O₂•⁻ pairs from the adsorbed O₂, the (photo)chemical reduction of WO₃ (i.e., the formation of Y_xW^{6-x}O₃, where Y refers to cations such as Li⁺, Na⁺, and H⁺) can shift the CB edge negatively (e.g., -0.15 V)³¹⁻³² and produce ROSs.

The effect of pH was further examined since the CB edge shifts upward (*i.e.*, -59 mV per pH)³³ with increasing pH, making the charge transfer more feasible (**Scheme 1**). As shown in **Figure 2b**, $[\text{As}^{\text{V}}]_{\text{max}}$ increased linearly with increasing pH (*approx.* 3-fold between pH 2 and 8) (*see Figure S4* for time-profiles of the production). An increase in pH to over ~ 9 resulted in gradual dissolution of WO_3 and hence the pH was not increased beyond this point. Notably, the protonated ROSs (OH^\bullet , HO_2^\bullet , and H_2O_2) undergo shifts in their redox potentials as much as the ΔCB edge (*i.e.*, -59 mV per pH), nullifying the positive effect of pH. On the other hand, the redox potential of $\text{O}_2^{\bullet-}$ is not influenced by pH due to the proton-free electron transfer. This suggests that $\text{O}_2^{\bullet-}$ can be responsible for As(III) oxidation, even though decoupling of $\text{O}_2^{\bullet-}$ and HO_2^\bullet is technically difficult.

The EPR spin-trapping technique with DMPO was employed to confirm the production of ROSs. As shown in **Figure 3a**, peaks associated with DMPO-OH and DMPO-OOH (virtually indistinguishable from those for DMPO- $\text{O}_2^{\bullet-}$)^{28,34} were found in the charged-TW filters (indicated by * and o, respectively); the peak intensity grew with time due to accumulation of the adducts. No specific peaks were observed for non-charged TW filters (**Figure S5**), indicating the formation of the adducts attributable to the ROSs produced in the charged TW filters. However, detection of the DMPO-OH adduct was rather unexpected because methanol (OH^\bullet scavenger) did not influence the As(III) oxidation kinetics (**Figure 2a**). Hence, SOD was added to the DMPO solution to re-confirm the production of $\text{O}_2^{\bullet-}$ (or $\text{HO}_2^\bullet/\text{O}_2^{\bullet-}$ pair) in charged TW filters.³⁰ As expected, peaks of the DMPO-OOH adduct vanished (**Figure 3b**); interestingly, peaks of the DMPO-OH adduct disappeared as well. The same behavior of both adducts can be attributed to the transformation of $\text{HO}_2^\bullet/\text{O}_2^{\bullet-}$ pair into

OH• via HOOH (R6-R8).³⁵ Removal of the former by SOD inhibits HOOH formation and consequently OH• formation.



However, H₂O₂ was not found in the filtered solutions regardless of the presence of As(III), even though its formation was thermochemically possible ($E^0(\text{O}_2/\text{H}_2\text{O}_2) = +0.695$ V).²⁶ It appears that the presence of As(III) inhibits the formation of HOOH (R6 and R7) due to the preferential reaction with the HO₂•/O₂•⁻ pair (R3 and R5), whereas HOOH decomposed into OH• in the absence of As(III) (R8). HO₂•/O₂•⁻ pairs can be indirectly produced from the decomposition of H₂O₂ via electron withdrawal from the O–O bond;³⁶ yet the pathway appeared to play a minor role in the process. To examine the possible effect of H₂O₂, As(III) solutions with various concentrations of H₂O₂ (0.01–0.1 mM) were passed through the *non-charged* TW (**Figure S6**). As(V) production increased with increasing H₂O₂ concentration; [As^V]_{max} for a H₂O₂ concentration at 0.01–0.02 mM was similar as that for the charged TW without added H₂O₂. This suggests that the pre-charging can have the same effect as H₂O₂ concentrations of 0.01 and 0.02 mM *only if* H₂O₂ is involved in the As(III) oxidation.

Storing charges in TiO₂/WO₃ composite membrane filters.

We have examined the primary roles of TiO₂ and WO₃ in photocharging-discharging processes. **Figure 4** shows the XPS spectra of W4f and Ti2p bands in TW membrane filters before and after photocharging. Obviously, the photocharging shifted the W 4f bands (W 4f_{5/2}

at ~ 36.7 eV and W $4f_{7/2}$ at ~ 34.7 eV) to a lower binding energy region by 0.5 eV. The W4f bands in the used TW filter (*i.e.*, discharged one) shifted back to the original binding energy. Such a reversible shift in the W4f band was found in the repeated As(III) oxidation cycles (*see Figure 7*). On the other hand, the Ti 2p bands insignificantly shifted ($\Delta 0.1$ eV) in the photocharging-discharging cycles. This indicates that the Ti^{4+} state was nearly unchanged, whereas the $W^{6+/(6-x)+}$ redox reaction occurred reversibly in the photocharging-discharging cycles. It appears that the photogenerated electrons are quickly transferred from TiO_2 to the interfacial O_2 and/or WO_3 , because the CB edge of TiO_2 is higher than the redox potential of O_2 and the CB edge of WO_3 . On the other hand, the CB edge of WO_3 is comparable to the O_2 redox potential and the unbalanced electron transfers between TiO_2/WO_3 (fast transfer) and WO_3/O_2 (slow transfer) should result in the electron accumulation in WO_3 (*i.e.*, formation of the $W^{(6-x)+}$ state) during the photocharging period. In the discharging period, the electron-accumulated WO_3 transfers the electrons to interfacial O_2 , shifting the $W^{(6-x)+}$ state to the W^{6+} state.

With this knowledge in mind, we attempted to optimize the synthesis of TW membrane filters and examine their applicability. **Figure 5a** shows the As(V) production using TW filters (pre-charged with UV254 and AM 1.5 light for 1 h) as a function of the weight ratio of TiO_2 and WO_3 (*see Figure S7* for time-profiles of the production). The UV254-charged TiO_2 filters without WO_3 (*i.e.*, TW 100) showed no activity toward As(III) oxidation in the dark. As the WO_3 fraction increased, the As(V) production increased rather linearly; however, with 100% WO_3 (TW 0), As(V) production decreased significantly. The highest activity of TW25 ($TiO_2/WO_3 = 1/3$) was found in the case of AM 1.5 light (*e.g.*, TW 25 vs. TW 50) as well. A large fraction of WO_3 can lead to broad absorption of AM 1.5 light

due to a narrower bandgap ($E_g \sim 2.7$ eV; $\lambda < \sim 450$ nm) than E_g of TiO_2 ($E_g \sim 3.2$ eV; $\lambda < 400$ nm, **Figure 5a inset**). However, the effect of TiO_2/WO_3 ratio cannot be simply explained in terms of the light absorption alone, because TW 25 was superior to TW 50 even when pre-charged with UV 254 (fully absorbed by both TiO_2 and WO_3). The significantly low activities of TW 0 (*i.e.*, 100% WO_3) and TW 100 (*i.e.*, 100% TiO_2) further suggest that both TiO_2 and WO_3 are essential as a supplier of photogenerated electrons and a reservoir, respectively. Hence, when the former role is limited, for example, by replacing TiO_2 with photo-inactive SiO_2 (*i.e.*, SiO_2/WO_3), then As(III) oxidation is significantly inhibited. In addition, if the role of the latter is removed, for example, using SiO_2 instead of WO_3 (*i.e.*, $\text{TiO}_2/\text{SiO}_2$), then As(III) oxidation does not proceed (**Figure S8**).

An increase in photocharging time also can enhance As(V) production for a fixed TW ratio (*i.e.*, TW 50). As shown in **Figure 5b**, As(V) production increased with increasing photocharging time (*i.e.*, $[\text{As}^{\text{V}}_{\text{max}}] \sim 0.3$ μmol in ~ 3 h; see **Figure S9** for time-profiles). As the photocharging continued, a light pale yellowish TW filter turned greenish blue in color (**Figure 5b inset**) due to reduction of W^{6+} to $\text{W}^{(6-x)+}$ in the WO_3 . The reduced state of the TW filter was stable in the absence of suitable interfacial electron acceptors (*e.g.*, O_2 , Cr(VI), and methylene blue).⁷ Time-resolved photoluminescence emission decay spectra (**Figure 5b inset**) further revealed that a photocharged TW filter showed a two-fold longer decay lifetime (τ) than that of a non-charged TW filter ($\tau \sim 14$ and 33 ns for non-charged and charged TW filters, respectively). It appears that the photo-charging creates trap sites, where the photogenerated electrons are gradually transferred to interfacial O_2 .

We attempted to quantitatively estimate the stored charge-to-As(III) oxidation efficiency ($\phi_{\text{sc}} = \phi_{\text{pc}} / \phi_{\text{ps}}$; see Eq. 4) of TW filters (pre-charged with UV 254 for 1 h). To do

this, TiO_2 was assumed to have no contribution to the charge storage. The maximum charge storage capacity of TW was dependent on the weight fraction of WO_3 (maximum 115 mAh g^{-1} when a single charge is stored in the form of HWO_3). The maximum photon-to-charge storage efficiency (ϕ_{ps} , as shown in Eq. 1) of WO_3 (i.e., TW 0) was $\sim 4.5\%$ and linearly decreased with increasing TW ratios (i.e., decreasing WO_3 fraction) (**Figure 6a**). In addition, the overall photoconversion efficiency (ϕ_{pc} ; see Eq. 3) was estimated, even though all As(III) oxidation reactions were performed in the dark. ϕ_{pc} was found to be less than 1%, and TW 25 exhibited the highest value (**Figure 6b**). This value (estimated in the dark) must be distinguished from the conventional photoconversion efficiency estimated under continuous irradiation. For example, TW 25 can drive As(III) oxidation in the dark with $\sim 0.65\%$ of incident photons (irradiated for 1 h). The highest ϕ_{pc} value for TW 25 suggests that the storage ability of WO_3 is critical. Based on the as-obtained ϕ_{ps} and ϕ_{pc} values, ϕ_{sc} could be estimated (**Figure 6c**). Although WO_3 alone (TW 0) exhibited ϕ_{sc} of $\sim 2.5\%$, significantly higher ϕ_{sc} values (15–20%) were observed for TiO_2 and WO_3 heterojunctions. The presence of TiO_2 should contribute to the charge transfer processes (i.e., generation, separation, and injection) and make WO_3 more reduced, which shifts the Fermi level of WO_3 and produces ROSs more effectively.

Finally, the maximum capacity of a 1 h-singly charged TW 50 filter for As(III) oxidation was examined. For this, a freshly prepared aqueous feed solution of As(III) was refilled after a previous cycle and passed through the same TW filter without additional charging. The As(V) production decreased gradually and completely disappeared in the fourth recycling (**Figure 7a**). The 1 h-singly charged TW 50 filter was estimated to oxidize a

total of $\sim 0.25 \mu\text{mol}$ of As(III). On the other hand, recharging of TW in each cycle recovered and maintained the catalytic activities of As(III) oxidation and Cr(VI) reduction (**Figure 7b** and **S10**, respectively). Reversible change in the color and shift in the XPS W4f band of TW filters (**Figure 4**) confirm that TW filters are stable and recyclable. This indicates that i) the gradual deactivation can be attributed to the consumption of electrons stored in the TW during the multiple uses and ii) the TW filter system can be easily reused after a simple recharging process without the need of recovery of the catalysts during repeated use. The same crystalline structure (monoclinic for WO_3 and mixed anatase/rutile for TiO_2) between photocharged and discharged TW filters further confirms the durability (**Figure S11**). For comparison, TiO_2 and WO_3 -mixed suspension systems were tested for As(III) oxidation under the same conditions as the TW filter system (**Figure S12**). The initial activity of the suspension was higher than that of the filter due to agitation-enhanced O_2 diffusion. However, a larger As(V) was produced in the filter system in the latter stage because a firm interparticle contact of TiO_2 and WO_3 was created in the filter whereas the suspension system underwent segregation of TiO_2 and WO_3 .

In summary, pre-charged TiO_2 and WO_3 (TW)-embedded inorganic membrane filters are demonstrated to be capable of oxidizing As(III) to As(V) under ambient dark conditions without any auxiliary chemical additives. The electrons accumulated in the TW composite filters during the charging period are transferred to interfacial O_2 , effectively forming ROSs, represented by HO_2^\bullet and $\text{O}_2^{\bullet-}$. The involvement of these species was confirmed with the corresponding quenchers and spin-trapping reagents; although not identified, H_2O_2 appeared to indirectly contribute to As(III) oxidation. The pre-charging time and TW ratios significantly influence the As(III) oxidation; the latter is particularly critical because WO_3

contributes to not only charge generation but also charge storage. The charged TW membrane system can be reused after recharging without disassembling the catalyst membrane. The proposed As(III) oxidation process using the proposed system is applicable to and environmentally benign in the continuous treatment of As(III)-contaminated water during periods of unavailability of sunlight (e.g., cloudy and night-time conditions).

Acknowledgements

This research was partly supported by the National Research Foundation of Korea (2019R1A2C2002602, 2018R1A6A1A03024962, and 2019M1A2A2065616). We are grateful to the Global Research Laboratory (GRL) Program (2014K1A1A2041044) through the National Research Foundation, Korea. This publication was made possible by a grant from the Qatar National Research Fund under its National Priorities Research Program (NPRP 10-1210-160019).

Supporting Information Available.

Digital photo and absorption spectra of TW before and after photocharging (Fig. S1), Photo and scheme of a once-through filtration system (Fig. S2), Time-changes of the amounts of Cr(III) and Cr(VI) (Fig. S3), Effect of initial solution pH on As(III) oxidation (Fig. S4), Time-changes in the EPR spectra with non-charged TW filters (Fig. S5), Effect of H₂O₂ on As(III) oxidation (Fig. S6), Time profiles of As(III) oxidation by charged TW membrane with different TW ratios (Fig. S7), Time profiles of As(III) oxidation on TiO₂/WO₃, TiO₂/SiO₂, and WO₃/SiO₂ filters (Fig. S8), Effect of photocharging time of TW on As(III) oxidation (Fig.

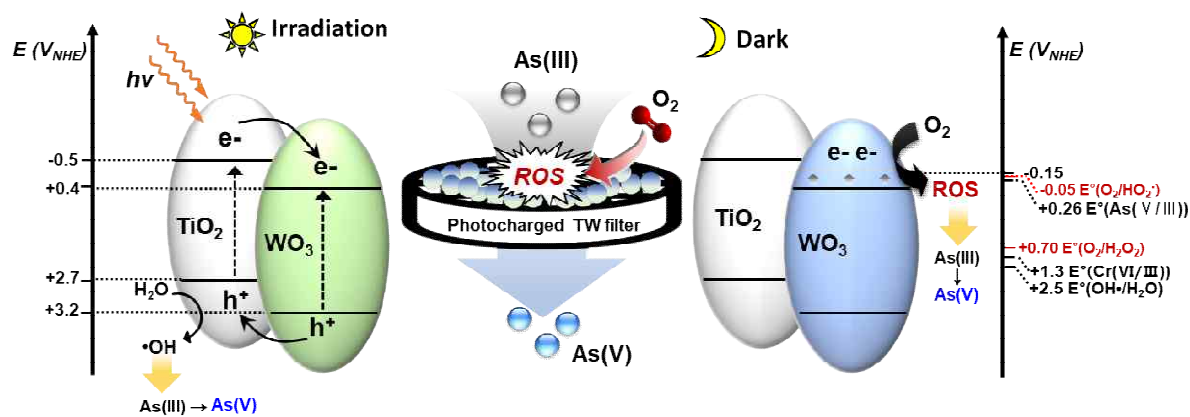
S9), Repeated runs of Cr(VI) reduction using TW filter photocharged every 3 h (Fig. S10), XRD patterns of TW filters as-synthesized, photocharged, discharged, and re-photocharged (Fig. S11), Time profiles of As(III) oxidation using membrane filter and suspension system of TW 25 (Fig. S12). This information is available free of charge via the Internet at <http://pubs.acs.org/>.

References

1. Hoffmann, M. R.; Martin, S. T.; Choi, W.; Bahnemann, D. W., Environmental applications of semiconductor photocatalysis. *Chem. Rev.* **1995**, *95*, 69-96.
2. Park, H.; Kim, H.-i.; Moon, G.-h.; Choi, W., Photoinduced charge transfer processes in solar photocatalysis based on modified TiO₂. *Energy Environ. Sci.* **2016**, *9*, 411-433.
3. Park, H.; Park, Y.; Kim, W.; Choi, W., Surface modification of TiO₂ photocatalyst for environmental applications. *J. Photochem. Photobiol. C* **2013**, *15*, 1-20.
4. Loeb, S. K.; Alvarez, P. J. J.; Brame, J. A.; Cates, E. L.; Choi, W.; Crittenden, J.; Dionysiou, D. D.; Li, Q.; Li-Puma, G.; Quan, X.; Sedlak, D. L.; Waite, T. D.; Westerhoff, P.; Kim, J. H., The technology horizon for photocatalytic water treatment: Sunrise or sunset? *Environ. Sci. Technol.* **2019**, *53*, 2937-2947.
5. Park, H.; Bak, A.; Jeon, T. H.; Kim, S.; Choi, W., Photochargeable and dischargeable TiO₂ and WO₃ heterojunction electrodes. *Appl. Catal. B* **2012**, *115-116*, 74-80.
6. Han, D. S.; Elshorafa, R.; Yoon, S. H.; Kim, S.; Park, H.; Abdel-Wahab, A., Sunlight-charged heterojunction TiO₂ and WO₃ particle-embedded inorganic membranes for night-time environmental applications. *Photochem. Photobiol. Sci.* **2018**, *17*, 491-498.
7. Kim, S.; Park, H., Sunlight-harnessing and storing heterojunction TiO₂/Al₂O₃/WO₃ electrodes for night-time applications. *RSC Adv.* **2013**, *3*, 17551-17558.
8. Kim, S.; Park, Y.; Kim, W.; Park, H., Harnessing and storing visible light using a heterojunction of WO₃ and CdS for sunlight-free catalysis. *Photochem. Photobiol. Sci.* **2016**, *15*, 1006-1011.
9. Ngaotrakanwiat, P.; Tatsuma, T.; Saitoh, S.; Ohko, Y.; Fujishima, A., Charge-discharge behavior of TiO₂-WO₃ photocatalysis systems with energy storage ability. *Phys. Chem. Chem. Phys.* **2003**, *5*, 3234-3237.
10. Tatsuma, T.; Saitoh, S.; Ngaotrakanwiat, P.; Ohko, Y.; Fujishima, A., Energy storage of TiO₂-WO₃ photocatalysis systems in the gas phase. *Langmuir* **2002**, *18*, 7777-7779.
11. Tatsuma, T.; Saitoh, S.; Ohko, Y.; Fujishima, A., TiO₂-WO₃ photoelectrochemical anticorrosion system with an energy storage ability. *Chem. Mater.* **2001**, *13*, 2838-2842.

- 411 12. Mohamed, H. H.; Dillert, R.; Bahnemann, D. W., Reaction dynamics of the transfer
412 of stored electrons on TiO₂ nanoparticles: A stopped flow study. *J. Photochem. Photobiol., A*
413 **2011**, *217*, 271-271.
- 414 13. Mohamed, H. H.; Mendive, C. B.; Dillert, R.; Bahnemann, D. W., Kinetic and
415 mechanistic investigations of multielectron transfer reactions induced by stored electrons in
416 TiO₂ nanoparticles: A stopped flow study. *J. Phys. Chem. A* **2011**, *115*, 2139-2147.
- 417 14. Mohamed, H. H.; Dillert, R.; Bahnemann, D. W., TiO₂ nanoparticles as electron
418 pools: Single- and multi-step electron transfer processes. *J. Photochem. Photobiol., A* **2012**,
419 *245*, 9-17.
- 420 15. Zhao, D.; Chen, C.; Yu, C.; Ma, W.; Zhao, J., Photoinduced electron storage in
421 WO₃/TiO₂ nanohybrid material in the presence of oxygen and postirradiated reduction of
422 heavy metal ions. *J. Phys. Chem. C* **2009**, *113*, 13160-13165.
- 423 16. Karagas, M. R.; Gossai, A.; Pierce, B.; Ahsan, H., Drinking water arsenic
424 contamination, skin lesions, and malignancies: A systematic review of the global evidence.
425 *Cur. Environ. Health Rep.* **2015**, *2*, 52-68.
- 426 17. Korte, N. E.; Fernando, Q., A review of arsenic(III) in groundwater. *Crit. Rev.*
427 *Environ. Control* **1991**, *21*, 1-39.
- 428 18. Kim, D.-h.; Bokare, A. D.; Koo, M. s.; Choi, W., Heterogeneous catalytic oxidation
429 of As(III) on nonferrous metal oxides in the presence of H₂O₂. *Environ. Sci. Technol.* **2015**,
430 *49*, 3506-3513.
- 431 19. Moon, G.-h.; Kim, D.-h.; Kim, H.-i.; Bokare, A. D.; Choi, W., Platinum-like
432 behavior of reduced graphene oxide as a cocatalyst on TiO₂ for the efficient photocatalytic
433 oxidation of arsenite. *Environ. Sci. Technol. Lett.* **2014**, *1*, 185-190.
- 434 20. Choi, W.; Yeo, J.; Ryu, J.; Tachikawa, T.; Majima, T., Photocatalytic oxidation
435 mechanism of As(III) on TiO₂: Unique role of As(III) as a charge recombinant species.
436 *Environ. Sci. Technol.* **2010**, *44*, 9099-9104.
- 437 21. Lenoble, V.; Deluchat, V.; Serpaud, B.; Bollinger, J.-C., Arsenite oxidation and
438 arsenate determination by the molybdenum blue method. *Talanta* **2003**, *61*, 267-276.
- 439 22. Jeong, H. W.; Chae, W.-S.; Song, B.; Cho, C.-H.; Baek, S.-H.; Park, Y.; Park, H.,
440 Optical resonance and charge transfer behavior on patterned WO₃ microdisc arrays. *Energy*
441 *Environ. Sci.* **2016**, *9*, 3143-3150.
- 442 23. Kang, U.; Park, H., A facile synthesis of CuFeO₂ and CuO composite photocatalyst
443 films for production of liquid formate from CO₂ and water over a month. *J. Mater. Chem. A*
444 **2017**, *5*, 2123-2131.
- 445 24. Rahn, R. O.; Stefan, M. I.; Bolton, J. R.; Goren, E.; Shaw, P.-S.; Lykke, K. R.,
446 Quantum yield of the iodide-iodate chemical actinometer: Dependence on wavelength and
447 concentration. *Photochem. Photobiol.* **2003**, *78*, 146-152.
- 448 25. Chen, Z.; Peng, Y.; Liu, F.; Le, Z.; Zhu, J.; Shen, G.; Zhang, D.; Wen, M.; Xiao, S.;
449 Liu, C.-P.; Lu, Y.; Li, X., Hierarchical nanostructured WO₃ with biomimetic proton channels
450 and mixed ionic-electronic conductivity for electrochemical energy storage. *Nano Lett.* **2015**,
451 *15*, 6802-6808.
- 452 26. Lide, D. R., *CRC Handbook of Chemistry and Physics*. 90th ed.; CRC Press: New
453 York, 2009.

27. Buxton, G. V.; Greenstock, C. L.; Helman, W. P.; Ross, A. B., Critical review of rate constants for reactions of hydrated electrons, hydrogen atoms and hydroxyl radicals in aqueous solution. *J. Phys. Chem. Ref. Data* **1988**, *17*, 513-886.
28. Bielski, B. H. J.; Cabelli, D. E.; Arudi, R. L.; Ross, A. B., Reactivity of HO_2/O_2^- radicals in aqueous solution. *J. Phys. Chem. Ref. Data* **1985**, *14*, 1041-1100.
29. Sawyer, D. T.; Valentine, J. S., How super is superoxide? *Acc. Chem. Res.* **1981**, *14*, 393-400.
30. Hayyan, M.; Hashim, M. A.; AlNashef, I. M., Superoxide ion: Generation and chemical implications. *Chem. Rev.* **2016**, *116*, 3029-3085.
31. Paik, T.; Cargnello, M.; Gordon, T. R.; Zhang, S.; Yun, H.; Lee, J. D.; Woo, H. Y.; Oh, S. J.; Kagan, C. R.; Fornasiero, P.; Murray, C. B., Photocatalytic hydrogen evolution from substoichiometric colloidal WO_{3-x} nanowires. *ACS Energy Lett.* **2018**, *3*, 1904-1910.
32. Yousaf, A. B.; Imran, M.; Zaidi, S. J.; Kasak, P., Highly efficient photocatalytic Z-scheme hydrogen production over oxygen-deficient WO_{3-x} nanorods supported $\text{Zn}_{0.3}\text{Cd}_{0.7}\text{S}$ heterostructure. *Sci. Rep.* **2017**, *7*, 6574.
33. Finklea, H. O., *Semiconductor Electrodes*. Elsevier: Amsterdam, 1988.
34. Buettner, G. R., On the reaction of superoxide with DMPO/OOH. *Free Rad. Res. Comms.* **1990**, *10*, 11-15.
35. Park, Y.; Kim, C.; Kim, M.; Kim, S.; Choi, W., Ambient-temperature catalytic degradation of aromatic compounds on iron oxide nanorods supported on carbon nanofiber sheet. *Appl. Catal. B* **2019**, *259*, 118066.
36. Arends, I. W. C. E.; Sheldon, R. A., Recent developments in selective catalytic epoxidations with H_2O_2 . *Top. Catal.* **2002**, *19*, 133-141.



Scheme 1. Illustration of As(III) oxidation reactions occurring in TiO₂/WO₃ (TW) membrane filters under irradiation (left) and in the subsequent dark periods (right). ROS refers to reactive oxygen species.

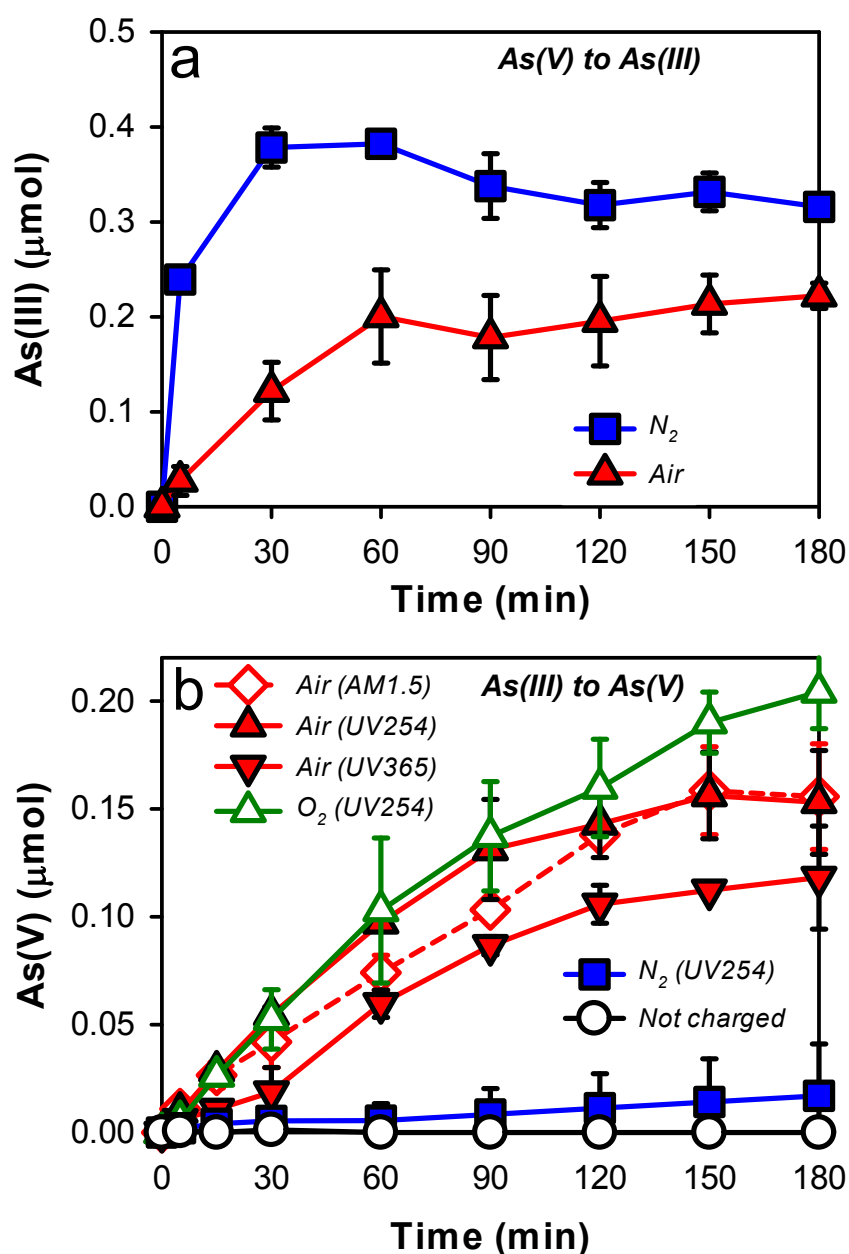


Figure 1. Time profiles of (a) As(III) production in aqueous solutions of As(V) (pH 5) and (b) As(V) production in aqueous solutions of As(III) (pH 5) under ambient conditions in the dark. In (a), air-equilibrated and N_2 -purged solutions with 0.1 mM As(V) solutions flowed at a rate of 0.5 mL min^{-1} through TW filters that were pre-charged for 1 h with UV 254 nm. In (b), 0.1 mM As(III) solutions that were equilibrated with air and purged with O_2 and N_2 were passed through pre-charged TW filters (for 1 h with UV 254 nm, UV 365 nm, and AM 1.5 light). While the solutions flowed, light was turned off. For comparison, the air-equilibrated As(III) solution flowed through non-charged TW.

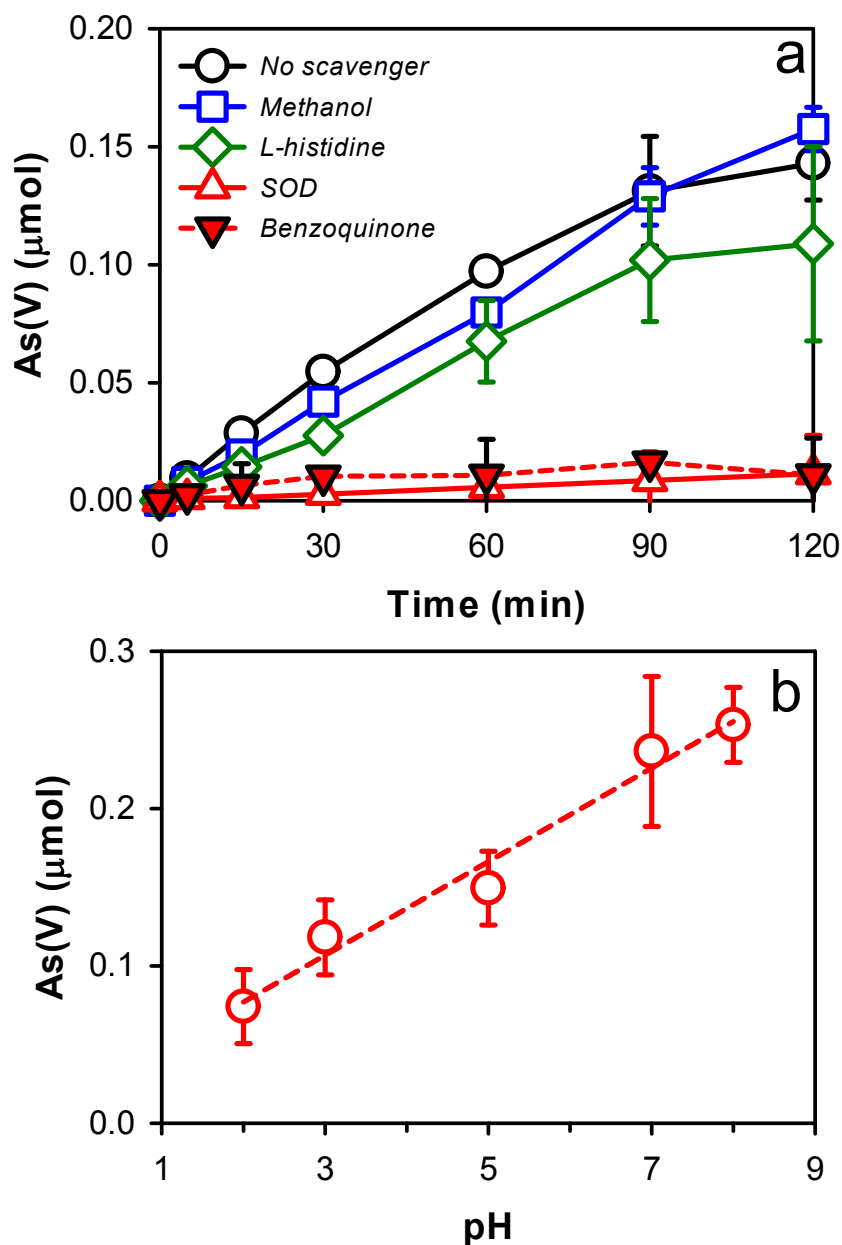
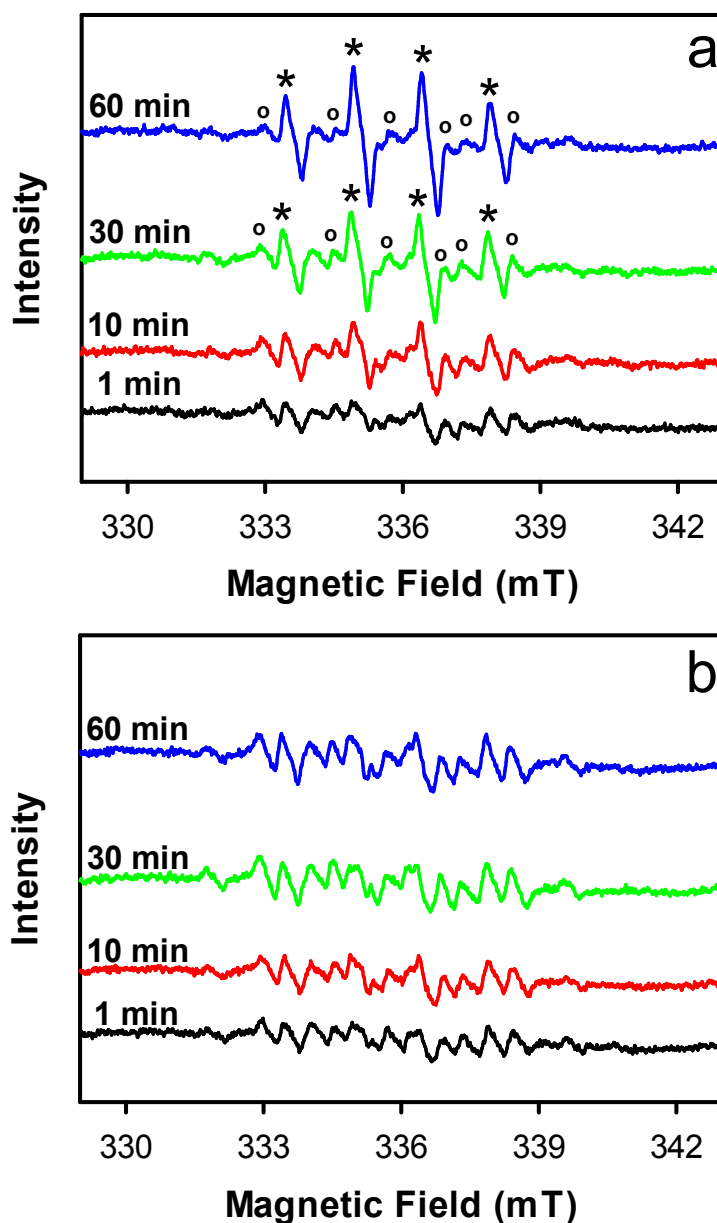


Figure 2. Effect of (a) ROS scavengers and (b) pH on the oxidation of As(III) to As(V). In (a), air-equilibrated As(III) solutions with methanol (100 mM), L-histidine (100 mM), SOD (55.11 mg L⁻¹), and *p*-benzoquinone (100 mM) as scavengers of $\cdot\text{OH}$, $^1\text{O}_2$, $\text{O}_2^{\cdot-}$, and HO_2^{\cdot} , respectively, flowed through pre-charged TW filters (for 1 h with UV 254). In (b), air-equilibrated As(III) solutions (0.1 mM) with various pH flowed through pre-charged TW filters.



498

499 **Figure 3.** Time profiles of EPR spectra of DMPO solutions (a) without and (b) with SOD
500 flowed through charged TW filters. Symbols “*” and “o” represent the peaks of DMPO-OH
501 and DMPO-OOH and adducts, respectively. [DMPO]₀ = 0.15 M; [SOD]₀ = 66.7 mg L⁻¹; TW
502 pre-charged for 2 h with UV254.

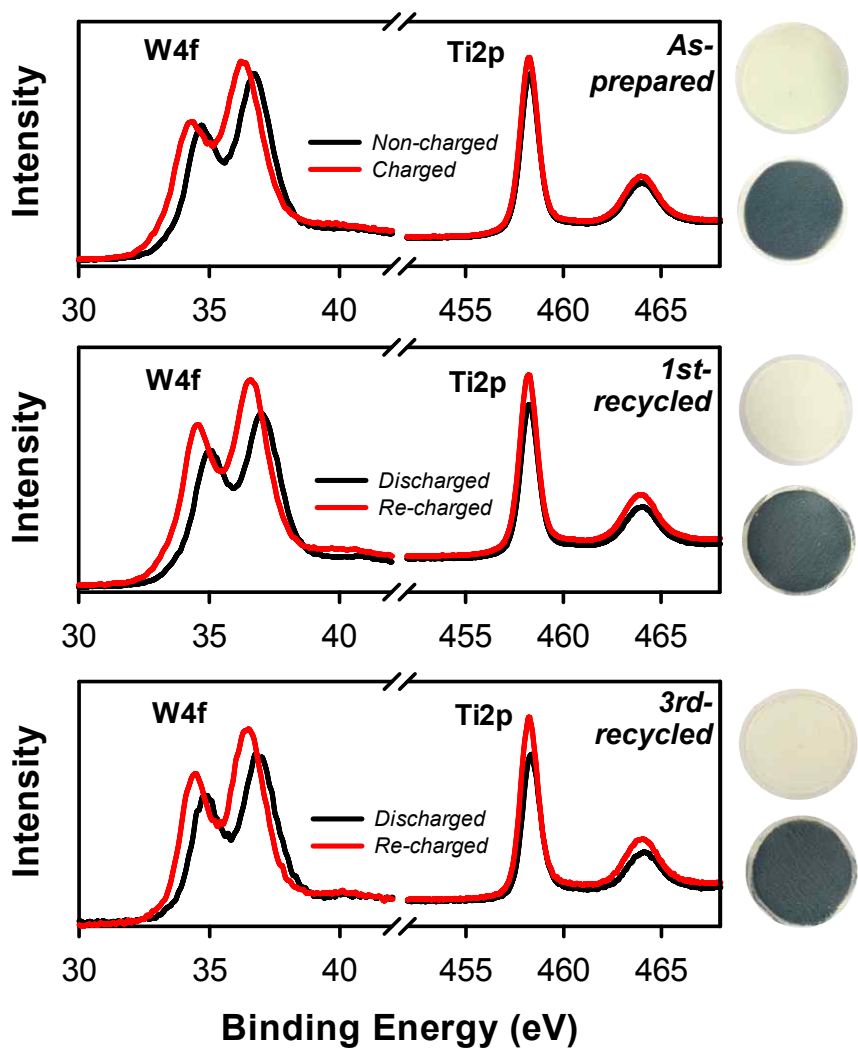
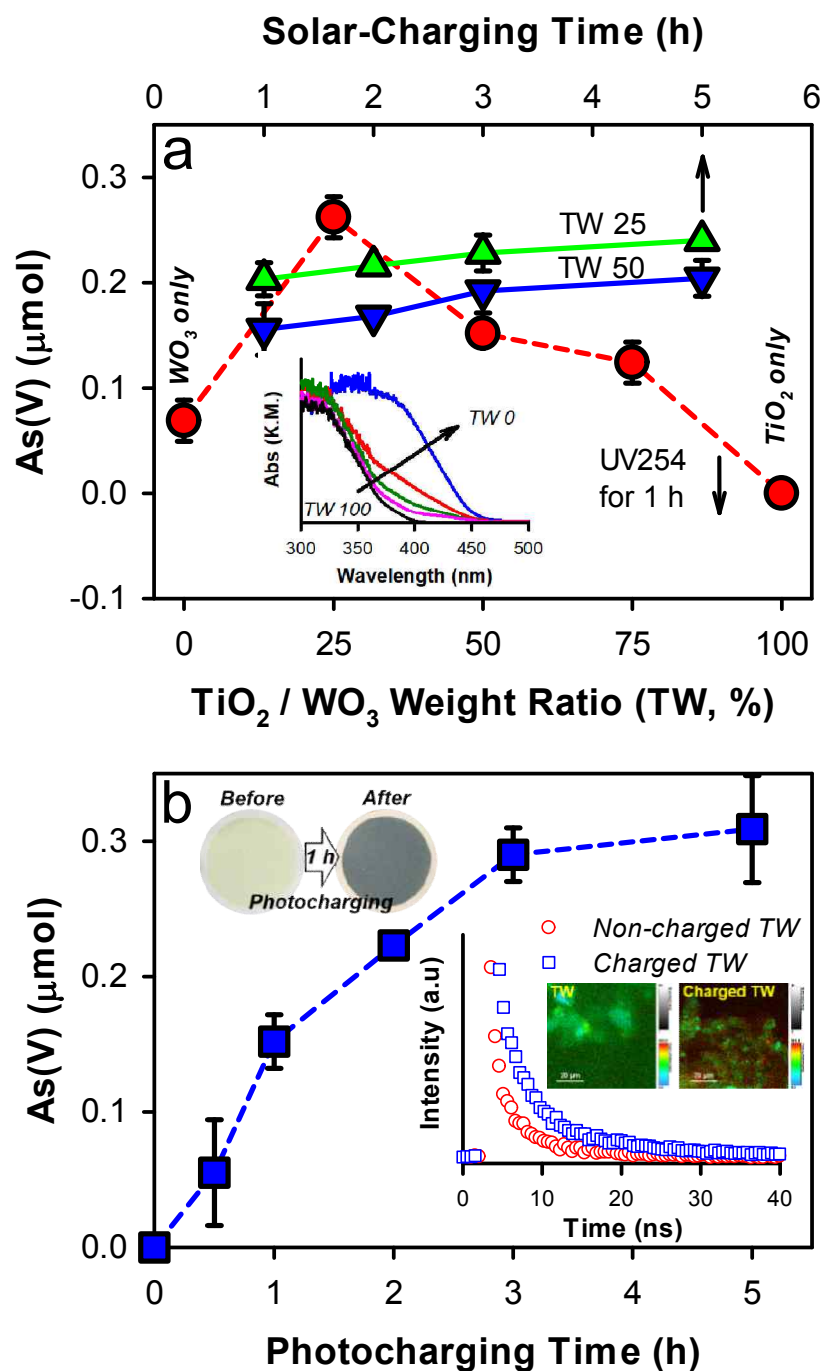


Figure 4. XPS spectra of W4f and Ti2p bands in as-prepared and recycled TW filters. The as-photocharged TW sample was used (i.e., discharged) for As(III) oxidation (see **Figure 7**); then the discharged TW sample was re-charged and reused (i.e., discharged) for As(III) oxidation. This recycle was repeated three times. The photos show the non-charged and charged TW filters (as-prepared), and discharged and recharged TW filters (1st and 3rd-recycled).



510

511 **Figure 5.** Effect of (a) TW weight ratio and (b) photocharging time on As(V) production (pH
 512 5). The inset in Figure 4b shows time-resolved photoluminescence emission spectra of TiO₂
 513 (T), WO₃ (W), and TiO₂/WO₃ (TW, non-charged and charged) films. Excited at $\lambda = 375$ nm.

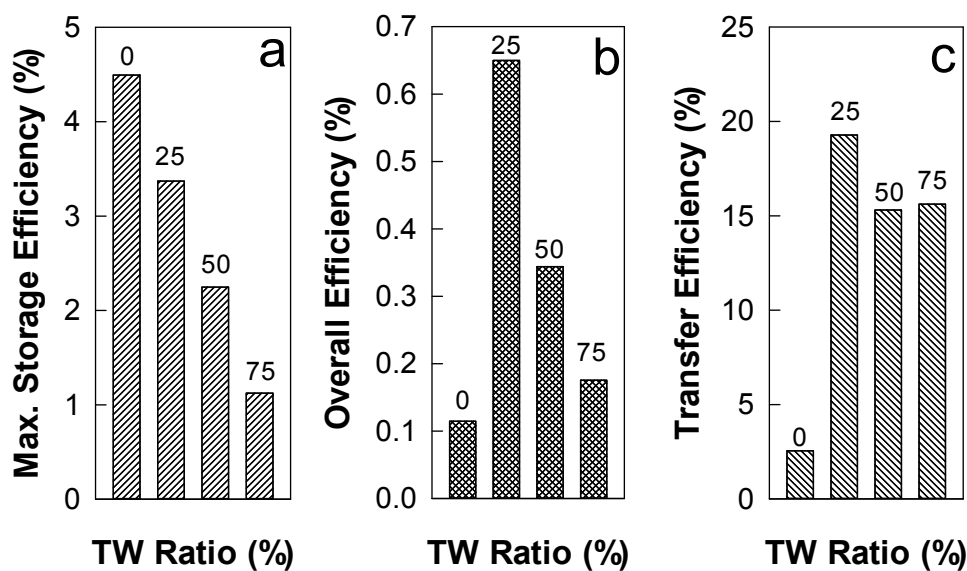
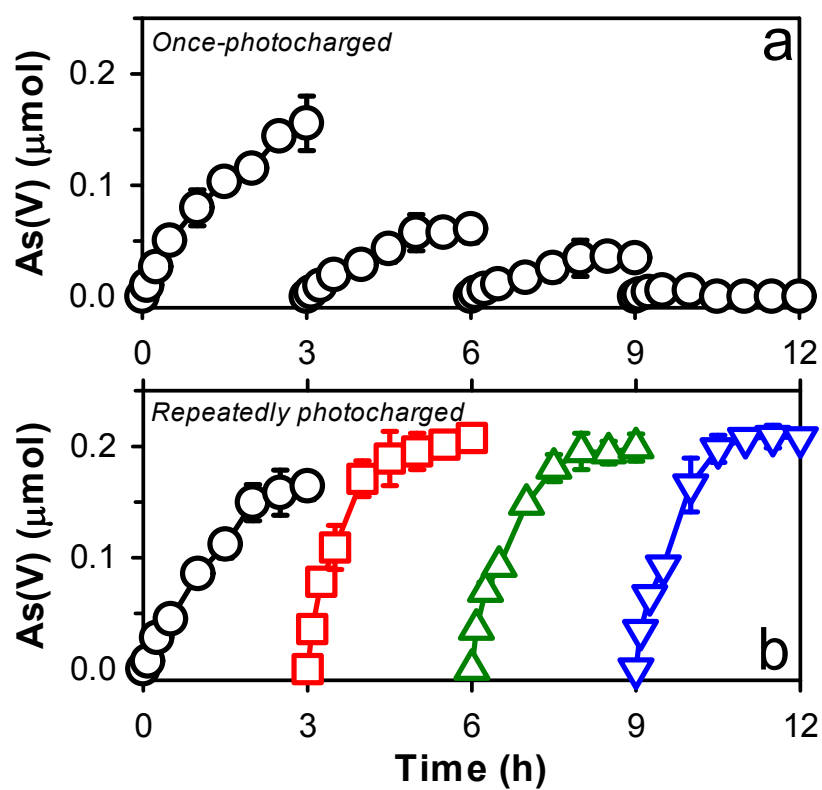


Figure 6. Effect of TiO_2 and WO_3 (TW) ratio on (a) the maximum charge storage efficiency, (b) the overall incident photon-to-As(III) oxidation efficiency in the dark, and (c) the stored charge-to-As(III) oxidation efficiency. TW filters were pre-charged with UV 254 nm for 1 h (approx. 5.23×10^{19} photons, 4% deviation).



519

520 **Figure 7.** Repeated runs of As(III) oxidation using (a) singly photocharged TW filter and (b)
521 TW filter photocharged every 3 h ($\text{pH}_i = 5.0$, $[\text{As(III)}]_i = 0.1 \text{ mM}$, air-equilibrated). The
522 photocharging time was 1 h with UV 254.

Table of Contents

